Scintillation properties of Pr-doped Li$_2$O-GeO$_2$ glasses

Noriaki Kawaguchi* and Takayuki Yanagida

Nara Institute of Science and Technology, 8916-5 Takayama-Cho, Ikoma, Nara 630-0192, Japan

We have investigated scintillation properties of the Pr-doped Li$_2$O-GeO$_2$ glasses. From the transmittance spectra, absorption bands due to 4f-4f transition of Pr^{3+} ions were observed. The samples showed the X-ray induced radioluminescence peaks originating from the 4f-4f transitions of the Pr^{3+} ion. The scintillation decay times were from 2.07 to 3.12 μs which are acceptable values for the scintillator. The Pr-doped Li$_2$O-GeO$_2$ glasses can be regarded as the candidate for the scintillation materials.

Keywords: Germanate glass, Scintillation, Radiation measurement.

Introduction

Scintillation materials, which show luminescence under radiation irradiation, play an important role in radiation detection applications. A lot of single crystal scintillators such as Tl:NaI, CsI:Tl, Bi$_4$Ge$_3$O$_{12}$, Ce:Lu$_2$SiO$_5$, and Ce:LuAlO$_3$ have been developed [1-4]. The Ce doped oxide scintillators having a non-hygroscopicity, a high light yield, and a fast decay time are mainly used in recent years. Although glass materials are generally more cost-effective than single crystal materials, there are few glass scintillators in practical use. The glass scintillators were intensively studied around 1960s [5-9], and scintillation characteristics of silicate, borosilicate, and phosphate glasses were investigated. It was found that its performance depends on the type of the glass former and silicate glasses exhibited excellent performance among them. The Ce-doped lithium silicate glass, that emits light by excitation energy due to nuclear reaction of ^{6}Li and neutron, has been put to practical use as a neutron scintillator [10-12]. The Ce-doped lithium silicate glass is still used as a standard neutron scintillator. Since there are few studies on scintillation properties of glasses except for silicate, borosilicate, and phosphate glasses, we are interested in the performance of the glasses containing lithium elements and other glass formers for the neutron scintillator application.

In this study, we focused on GeO$_2$ as the glass former for the scintillation materials. As the first choice of the dopant for scintillation materials, the Ce^{3+} ion is attractive. However, intense luminescence originating from 5d-4f transitions of the Ce^{3+} ion in germanate

glass have not been reported to the best of our knowledge. In the Ce-doped calcium gallium germanate glass, the Ce^{3+} luminescence have not been observed [13]. In addition, the Ce-doped BaO-Gd$_2$O$_3$-GeO$_2$ glass shows significantly lower luminosity than Ce-doped phosphate, borate, and silicate glasses [14]. From these results, we have assumed that the Ce ion is not a suitable dopant for the germanate glass. In the high energy physics and the nuclear medicine, fast scintillators such as the Ce-doped oxide materials with nanosecond order decay times are required. In the case of the other applications, scintillators with microsecond order decay times can be sufficiently used even for photon-counting type detectors; therefore, we studied another dopant for the germanate glass scintillator. Other than the Ce ion, the Pr^{3+} ion is one of the candidate for dopant because the Pr^{3+} ion can show fast luminescence with 5d-4f (nanosecond order decay time) and 4f-4f transitions (microsecond order decay time). In this study, we have investigated the scintillation properties of the Pr-doped 25Li$_2$O-75GeO$_2$ glasses in comparison with the non-doped and Ce-doped 25Li$_2$O-75GeO$_2$ glasses.

Experimental

The non-doped, Pr-doped, and Ce-doped 25Li$_2$O-75GeO$_2$ glasses were prepared using the conventional melt quenching technique. As the raw materials, high purity Li$_2$CO$_3$, GeO$_2$, Pr$_6$O$_{11}$, and CeO$_2$ powders were used. The powders were weighed in the stoichiometric compositions of 25Li$_2$O-75GeO$_2$ added with 0, 0.2, 0.5, 1.0, and 2.0 mol% of Pr^{3+} ions. The powders with the stoichiometric composition of 25Li$_2$O-75GeO$_2$ added with 0.5 mol% of Ce^{3+} ions were also prepared in a similar manner. The weighed powders were homogeneously mixed and melted by heating at 1000 ºC

*Corresponding author:
 Tel : +81-743-72-6144
 E-mail: n-kawaguchi@ms.naist.jp

for 30 min in aluminum crucibles with an electrical furnace (FTV-1700, FULL-TECH). The melted materials were poured on a stainless plate pre-heated at 300 ºC and then pressed by another stainless plate. All the obtained glasses were cut and mechanically polished to thickness of 1.0 mm.

To evaluate absorption bands of the samples, the in-line transmittance spectra of the Pr doped 25Li$_2$O-75GeO$_2$ glasses were measured in a wavelength range between 200 to 700 nm with 1 nm steps using a spectrophotometer (V670, JASCO). Photoluminescence (PL) excitation and emission maps and PL quantum yields of the samples were obtained using a PL quantum yield spectrometer (Quantaurus-QY; C11347, Hamamatsu Photonics). The spectral ranges of excitation and emission were 250-500 nm and 200-950 nm, respectively.

X-ray induced scintillation spectra of the samples were measured using an X-ray generator (W anode, 80 kV, 1.2 mA; XRB80P&N200X4550, Spellman High Voltage Electronics) and two types of CCD spectrometers having sensitivities in the different wavelength ranges. One of them is from UV to visible (DU-920-BU2NC, Andor Technology) and the other is from red to infrared (QEPro, Ocean Optics). The applied X-ray tube voltage and current were 80 kV and 1.2 mA, respectively. The system configuration is described in detail elsewhere [15]. X-ray induced scintillation decay curves of the Pr-doped samples were obtained by a time-correlated single photon counting system operated together with a pulse X-ray source (Hamamatsu Photonics) [16]. The obtained scintillation decay curves were fitted by the following equation:

$$I(t) = I(0)\ \exp(-t/t) + C \qquad (1)$$

where I(t) is the luminescence intensity as a function of time t, I(0) is luminescence intensity at t = 0, t is decay time and C is constant. The obtained scintillation decay times were compared to traditional scintillation materials.

Results and Discussion

The non-doped and Pr-doped 25Li$_2$O-75GeO$_2$ glasses were successfully obtained using the conventional melt quenching technique. Fig. 1 shows the samples that were illuminated by a white LED and an UV (254 nm) lump. All the samples are highly transparent, and the Pr-doped samples show yellow-green color while the non-doped sample is colorless. In addition, no cracks and inclusions are found in the samples by visual observation. Under UV irradiation, we observed orange luminescence from the Pr-doped samples. Since we could not observe luminescence from the non-doped sample under UV irradiation, it is considered that the Pr-doped samples showed extrinsic luminescence.
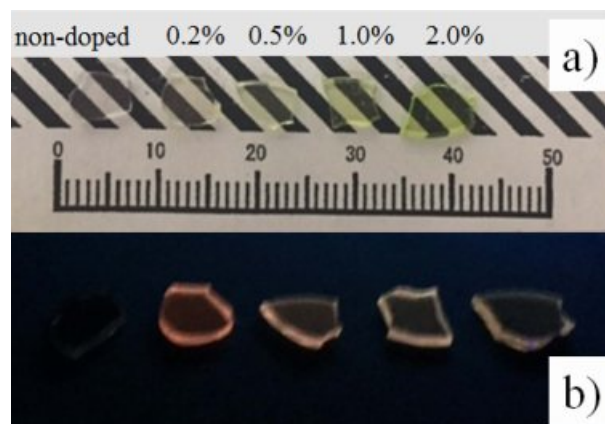
Fig. 2 shows the in-line transmittance spectra of the

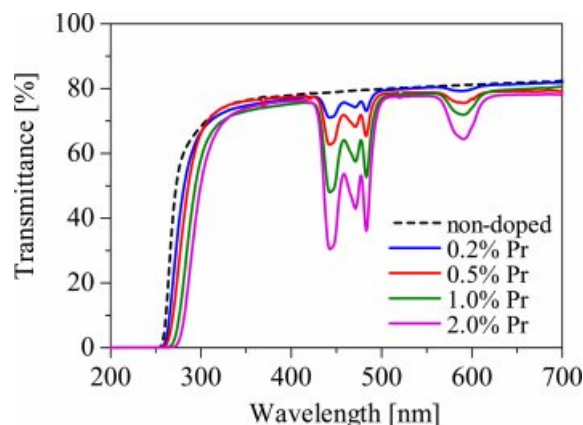**Fig. 1.** The non-doped and Pr-doped Li$_2$O-GeO$_2$ glasses.

Fig. 2. The transmittance spectra of the non-doped and Pr-doped Li$_2$O-GeO$_2$ glasses.

samples. The Pr-doped samples show absorption bands at around 440, 470, 480, and 590 nm that can be ascribed to 4f-4f transitions of the Pr^{3+} ion, while the non-doped sample shows no significant absorption bands. The absorption depth is prone to increase with increasing of the Pr concentration. The absorption edges of the Pr-doped samples shift to the longer wavelengths in comparison to that of the non-doped sample. It can be regarded as an influence of the absorption of the Pr^{3+} ions.

Fig. 3 shows the PL excitation and emission maps of the non-doped and 0.2% Pr-doped samples. When the excitation wavelength is from 430 to 500 nm, the 0.2 % Pr-doped sample shows emission peaks at around 490, 530, 610, and 650 nm while the non-doped sample shows no significant luminescence. Thus, the Pr-doped sample has excitation and emission bands that are not observed in the non-doped sample.

Fig. 4 shows the X-ray induced radioluminescence spectra of the non-doped and Pr-doped samples. The Pr-doped samples show the emission peaks at 490, 530, 610, 650, and 1050 nm while the non-doped sample shows no emission peaks. The intensity of the emission peak at around 1050 nm decreased with increasing of
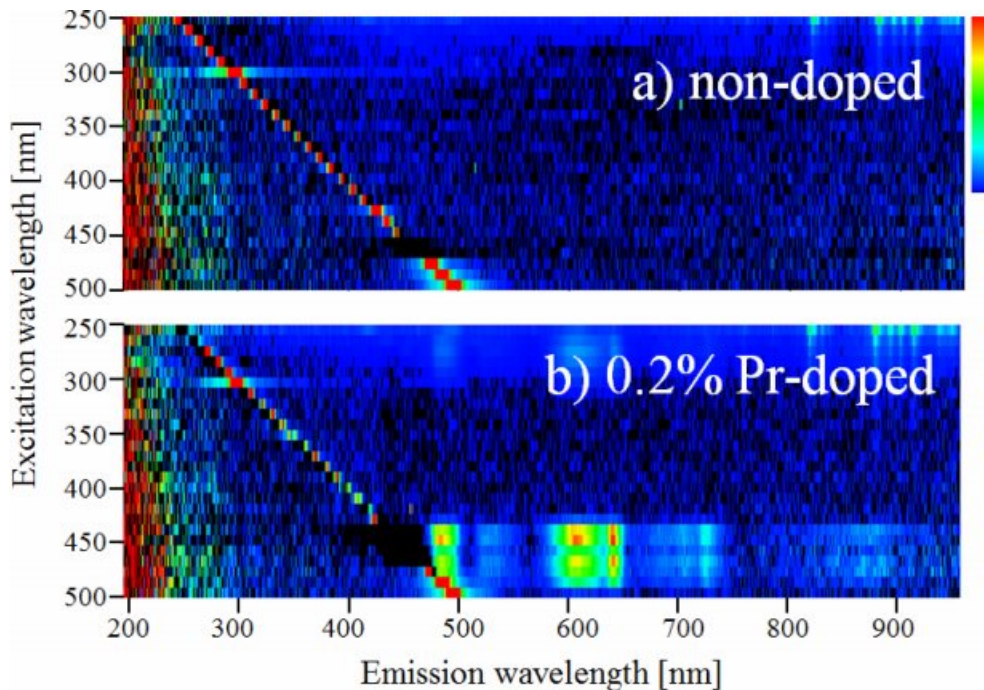
Fig. 3. The PL excitation and emission maps of the (a) non-doped and (b) 0.2% Pr-doped Li$_2$O-GeO$_2$ glasses.
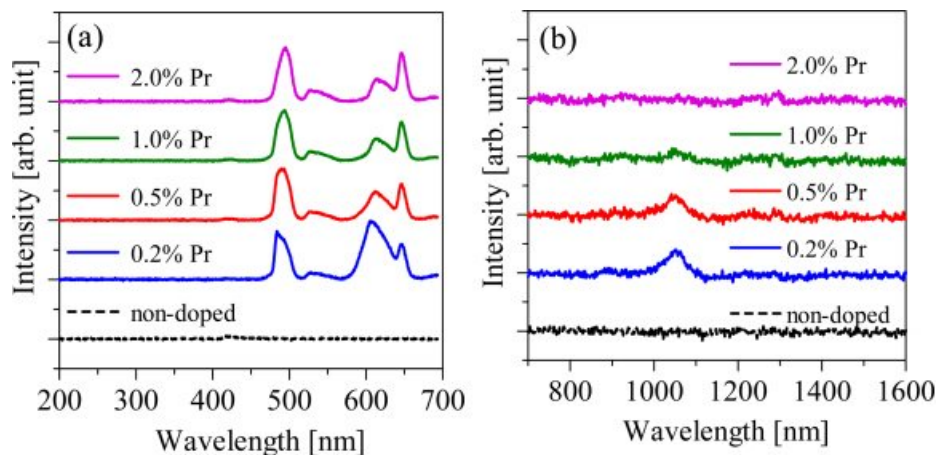

Fig. 4. The X-ray induced radioluminescence spectra of the non-doped and Pr-doped Li$_2$O-GeO$_2$ glasses in the wavelength ranges (a) from 200 to 700 nm and (b) from 700 to 1600 nm.

Pr concentration, and the 2.0 % Pr-doped sample shows no emission peaks at around 1050 nm. The cause for this tendency is considered to be due to the concentration quenching. The observed emission peaks in the PL maps and the X-ray induced radioluminescence spectra can be explained as the luminescence with the 4f-4f transition of Pr^{3+} ions. The emission peaks at 490, 530, 610, 650, and 1050 nm are ascribed to $^3P_0 \rightarrow {}^3H_4$, $^3P_0 \rightarrow {}^3H_5$, $^3P_0 \rightarrow {}^3H_6$, $^3P_0 \rightarrow {}^3H_6$, and $^1D_2 \rightarrow {}^3F_4$ transitions, respectively. Fig. 5 shows the X-ray induced radioluminescence spectrum and the visual appearance of the 0.5 % Ce-doped Li$_2$O-GeO$_2$ glass. The obtained Ce-doped Li$_2$O-GeO$_2$ glass looks transparent. On the other hand, emission peaks were not observed under X-ray irradiation. This result is consistent with previous

reports on other Ce-doped germanate glasses [13, 14]. From these results, the Pr^{3+} ion is considered to be the better dopant for the Li$_2$O-GeO$_2$ glass than the Ce^{3+} ion.

Fig. 6 shows the PL quantum yields of the samples in the emission wavelength range from 200 to 950 nm. The quantum yields of the Pr-doped samples are higher at around 450 and 470 nm of the excitation wavelengths. This is consistent with the absorption bands in transmittance spectra. When the excitation wavelength is 450 nm, the PL quantum yields of the 0.2, 0.5, 1.0, and 2.0 % Pr doped samples were 15.4, 12.0, 8.9, and 4.1 %, respectively. The 0.2 % Pr-doped sample shows the highest PL quantum yield among the samples. Fig. 7 shows the scintillation decay curves of the Pr-doped
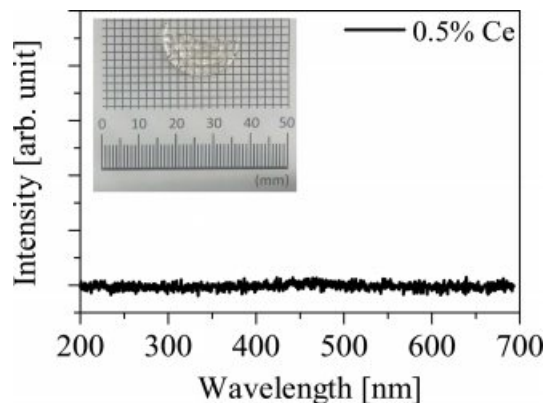
Fig. 5. The X-ray induced radioluminescence spectrum of the 0.5% Ce-doped Li_2O-GeO_2 glass in the wavelength range from 200 to 700 nm. The inset is the visual appearance of the 0.5% Ce-doped Li_2O-GeO_2 glass.

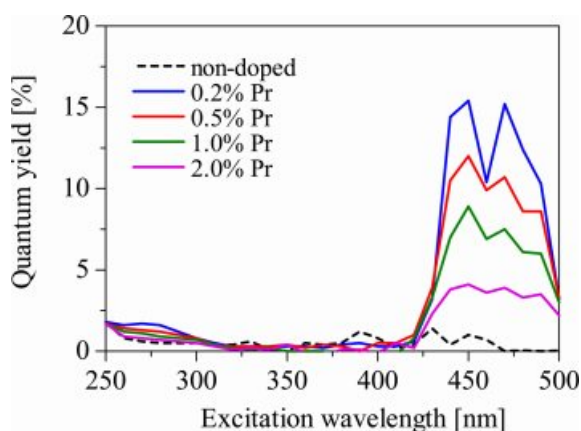**Fig. 6.** The PL quantum yields of the non-doped and Pr-doped Li_2O-GeO_2 glasses in the excitation wavelength range from 250 to 500 nm.

Fig. 7. The scintillation decay curves of the non-doped and Pr-doped Li_2O-GeO_2 glasses.

Table 1. The decay times of conventional neutron scintillators and the Pr-doped Li_2O-GeO_2 glasses.

Material	Decay time	Reference
Lithium glass GS20	75 ns	[10]
LiI:Eu	1400 ns	[10]
LiF/Ag:ZnS	> 1000 ns	[10]
Cs_2LiYCl_6	~ 1000 ns	[10]
$LiCaAlF_6$:Eu	~ 1.2 μs	[17-19]
LiF:W	43 μs	[20-22]
Pr doped Li_2O-GeO_2 glasses	2.07-3.12 μs	This work

samples. The scintillation decay curves can be fitted by single component exponential functions, and the estimated decay times of the 0.2, 0.5, 1.0, and 2.0 % Pr-doped samples were 3.12, 3.15, 2.78, and 2.07 μs. As the Pr concentration increased, the decay time becomes faster and the quantum yield becomes lower. It seems the typical behavior of the concentration quenching. Table 1 shows the decay times of conventional neutron scintillators and the Pr-doped Li_2O-GeO_2 glasses. Compared to conventional materials [10, 17-22], the Pr-doped Li_2O-GeO_2 glasses show acceptable decay times for the scintillator. Therefore, the luminescence with 4f-4f transitions of the Pr^{3+} ion can be potentially utilized for the neutron scintillator based on Li_2O-GeO_2 glasses.

Conclusion

We have investigated scintillation properties of the non-doped, Pr-doped, and Ce-doped $25Li_2O$-$75GeO_2$ glasses. All the glass samples were successfully obtained by the conv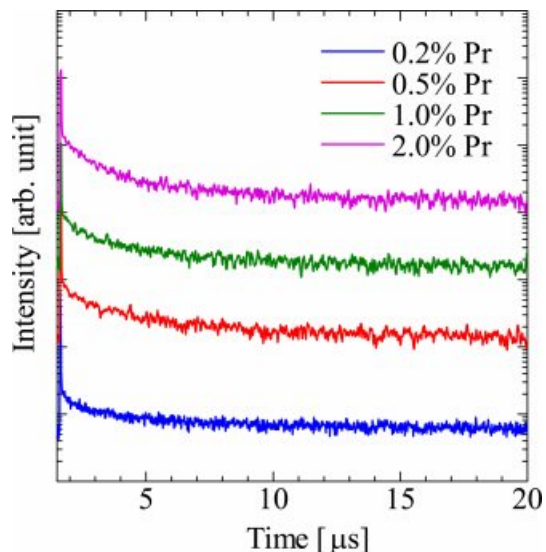entional melt quenching technique. From the transmittance spectra of the Pr-doped samples, we observed absorption bands due to the 4f-4f transition of Pr^{3+} ions. The emission peaks originating from the 4f-4f transition of the Pr^{3+} ions are observed in the Pr-doped samples under X-ray irradiation, while no emission peaks were observed in the non-doped and Ce-doped samples. The scintillation decay times were from 2.07 to 3.15 μs that are acceptable values for most of the scintillator applications. We have concluded that the Pr-doped Li_2O-GeO_2 glasses are the candidate for the scintillation materials.

References

1. G.F. Knoll, in "Radiation Detection and Measurement" (Wiley Press, 2010) p.219.
2. S.E. Derenzo, M.J. Weber, E. Bourret-Courchesne, and M.K. Klintenberg, J. Nucl. Instrum. Methods Phys. Res., Sect. A 505[1-2] (2003) 111-117.
3. C.W.E. Eijk, Phys. Med. Biol. 47 (2002) R85-R106.
4. T. Yanagida, Opt. Mater. 35 (2013) 1987-1992.
5. L.A. Wraight, D.H.C. Harris, and P.A. Egelstaff, J. Nucl. Instrum. Methods 33[2] (1965) 181-193.
6. H.O. Zetterström, S. Schwarz, and L.G. Strömberg, J. Nucl. Instrum. Methods 42[2] (1966) 277-282.
7. A.R. Spowart, J. Nucl. Instrum. Methods 75[1] (1969) 35-42.
8. E. Fort, J.L. Leroy, and J.P. Marquette, J. Nucl. Instrum. Methods 85[1] (1970) 115-123.
9. A.R. Spowart, J. Nucl. Instrum. Methods 82 (1970) 1-6.
10. C.W.E. van Eijk, A. Bessière A, and P. Dorenbos, J. Nucl. Instrum. Methods Phys. Res., Sect. A 529[1-3] (2004) 260-267.
11. C.W.E. van Eijk, J. Radiat. Meas. A 38[4-6] (2004) 337-342.
12. C.W.E. van Eijk, J. IEEE Trans. Nucl. Sci. 59[5] (2012) 2242-2247.
13. B.V. Padlyak and B. Kuklinski, J. Radiat. Meas. 38 (2004) 593-597.
14. J. Bei, G. Qian, X. Liang, S. Yuan, Y. Yang, and G. Chen, J. Mat. Res. Bull. 42[7] (2007) 1195-1200.
15. T. Yanagida, K. Kamada, Y. Fujimoto, H. Yagi, and T. Yanagitani, J. Opt. Mater. 35[12] (2013) 2480-2485.
16. T. Yanagida, Y. Fujimoto, T. Ito, K. Uchiyama, and K. Mori, J. Appl. Phys. Exp. 7[6] (2014) 062401.
17. N. Kawaguchi, T. Yanagida, A. Novoselov, K.J. Kim, K. Fukuda, A. Yoshikawa, M. Miyake, and M. Baba, Conference Record of the IEEE NSS/MIC, 1174-1176, Dresden, Germany, 2008.
18. T. Yanagida, N. Kawaguchi, Y. Fujimoto, K. Fukuda, Y. Yokota, A. Yamazaki, K. Watanabe, J. Pejchal, A. Uritani, T. Iguchi, and A. Yoshikawa, J. Opt. Mater. 33[8] (2011) 1243-1247.
19. T. Yanagida, A. Yamaji, N. Kawaguchi, Y. Fujimoto, K. Fukuda, S. Kurosawa, A. Yamazaki, K. Watanabe, Y. Futami, Y. Yokota, A. Uritani, T. Iguchi, A. Yoshikawa, and M. Nikl, J. Appl. Phys. Express 4[10] (2011) 106401.
20. B. Pritychenko, A. Da Silva, A. Smith, P. D. Barnes, and B. Sadoulet, J. Nucl. Instrum. Methods A 396[3] (1997) 371-373.
21. R Nowotny, J. Phys. Med. Biol. 49[12] (2004) 2599-2611.
22. N. Kawaguchi, N. Kawano, G. Okada, and T. Yanagida, Sens. Mater. 29 (2017) 1431-1438.